

Liver-Targeting and pH-Sensitive Sulfated Hyaluronic Acid Mixed Micelles for Hepatoma Therapy

This article was published in the following Dove Press journal:
International Journal of Nanomedicine

Zhi-peng Li^{1,*}
Gui-xiang Tian^{1,*}
Hong Jiang^{1,*}
Rui-yan Pan²
Bo Lian¹
Min Wang¹
Zhi-qin Gao¹
Bo Zhang²
Jing-liang Wu¹

¹School of Bioscience and Technology, Weifang Medical University, Weifang, Shandong, People's Republic of China;
²School of Pharmacy, Weifang Medical University, Weifang, Shandong, People's Republic of China

*These authors contributed equally to this work

Background: The tumor-targeting ability and pH-sensitive properties of intelligent drug delivery systems are crucial for effective drug delivery and anti-tumor therapy.

Methods: In this study, sHA-DOX/HA-GA mixed micelles were designed with the following properties: sulfated hyaluronic acid (sHA) was synthesized to block cell migration by inhibiting HAase; sHA-DOX conjugates were synthesized via pH-sensitive hydrazone bond to realize DOX-sensitive release. The introduction of HA-GA conjugate could improve active-targeting ability and cellular uptake.

Results: The results showed that the mixed micelles possessed a nearly spherical shape, nanoscale particle size (217.70 ± 0.89 nm), narrow size distribution ($PDI = 0.07 \pm 0.04$), negative zeta potential (-31.87 ± 0.61 mV) and pH-dependent DOX release. In addition, the sHA-DOX/HA-GA micelles exhibited concentration-dependent cytotoxicities against liver carcinoma cells (HepG2) and HeLa cells, and were shown to be effectively taken up by HepG2 cells by confocal microscopy analysis. Furthermore, the in vivo anti-tumor study showed that mixed micelles had a superior anti-tumor effect compared to that of free DOX. Further evidence obtained from the hematoxylin-eosin staining and immunohistochemistry analysis also demonstrated that sHA-DOX/HA-GA exhibited stronger tumor inhibition and lower systemic toxicity than free DOX.

Conclusion: The sHA-DOX/HA-GA mixed micelles could be a potential drug delivery system for anti-hepatoma therapy.

Keywords: hyaluronic acid, glycyrrhetic acid, hepatoma-targeting, pH-sensitive, micelles, anti-tumor therapy

Introduction

Liver cancer is one of the most common malignancies, with steadily increasing incidence globally. It has become the fourth leading cause of cancer-related deaths.^{1,2} Traditional chemotherapy is one of the main treatment approaches used for cancer therapy.^{3,4} Typical anti-cancer drugs, such as paclitaxel (PTX), doxorubicin (DOX), cisplatin (Pt), exhibit remarkable tumor inhibition, but these anti-cancer drugs are restricted in clinical applications due to their strong systemic toxicities, short half-times, non-specific targeting and vulnerability to multi-drug resistance (MDR).⁵⁻⁸

To overcome these limitations, intelligent drug delivery systems based on nano-scaled polymeric carriers, such as alginate micelles, hyaluronic acid micelles, and polyethylene glycol-phosphatidylethanolamine (PEG-PE) micelles, have been widely applied in anti-cancer therapy.⁹⁻¹¹ Hyaluronic acid (HA), a kind of nonsulfated glycosaminoglycan consisting of alternating units of D-glucuronic acid and N-acetyl-D-glucosamine, can serve as drug-loaded carriers due to many advantages, such as

Correspondence: Bo Zhang
School of Pharmacy, Weifang Medical University, Weifang, Shandong 261053, People's Republic of China
Email bozh315@163.com

Jing-liang Wu
School of Bioscience and Technology, Weifang Medical University, Weifang, Shandong 261053, People's Republic of China
Tel +86 536 846 2541
Email jlwu2008@163.com

favorable biocompatibility, non-immunotoxicity, and easy functional modification.^{12–14} HA polymers modified by hydrophobic ligands can be self-assembled into nano-sized micelles with a core-shell structure in aqueous media. These hydrophobic ligands can be different functional groups, such as poly(L-histidine) (PHis) and ceramide, or they can also be hydrophobic anti-cancer drugs such as paclitaxel, camptothecin, DOX, and cisplatin.^{15–17} However, high-molecular-weight HA polymers can be easily degraded by hyaluronidase (HAase) to form low-molecular-weight fragments, which could promote tumor proliferation and migration.¹⁸ In order to avoid this disadvantage, sulfated hyaluronic acid (sHA) was synthesized by introducing sulphation to the –OH groups of HA polymers and used to block degradation by HAase, thus inhibiting the proliferation, motility, and invasion of tumor cells.^{19–21} More recently, Lim et al demonstrated that sulfated HA can cause a decrease in angiogenesis, which may be used to treat angiogenesis-related diseases including solid tumors, wet age-related macular degeneration (wet-AMD) and retinitis pigmentosa.²²

To improve the selectivity and efficacy of anti-tumor drugs in liver cancer cells, a desirable strategy is to design liver-targeting nano-carriers modified by targeting moieties, such as sugars, antibodies, and various ligands.²³ Glycyrrhetic acid (GA), a pentacyclic triterpenoid, is one of the main bioactive components of licorice. It has been shown that GA receptors (GA-R) are highly expressed in liver cancer cells.²⁴ Therefore, GA-modified micelles could selectively target liver cancer cells and remarkably improve the accumulation of drugs in tumors.²⁵

In addition, the achievement of controlled release of the drugs is crucial for the creation of effective nano-carriers. One promising strategy is to design stimuli-responsive carriers, which are stable on physiological conditions but can be triggered to release drugs in the target region. Recently, many environmentally responsive nanoparticles have been prepared for anti-tumor therapy in which drug release would be triggered when environmental conditions, such as pH, temperature, redox, light, and magnetic fields change in vivo.^{26–28} Among these, pH-sensitive drug delivery systems based on an acid-labile hydrazone bond are frequently applied. Hydrazone bonds can remain stable under physiological pH but disintegrate in lysosomal pH (~5.5), resulting in rapid drug release.²⁹

In previous studies, DOX has been widely used as a model anticancer drug for the treatment of many solid tumors, such as in liver, lung, bladder, prostate and breast cancers. DOX blocks the proliferation of tumor cells through inhibition of

DNA and protein synthesis.^{30–32} Moreover, DOX could be tracked easily due to its self-fluorescence.³³ In this work, sHA-DOX/HA-GA mixed micelles were designed with the following properties (Figure 1): First, sulfated hyaluronic acid (sHA) was synthesized to block cell migration by inhibiting HAase. Second, sHA-DOX conjugates were synthesized via a pH-sensitive hydrazone bond to realize DOX-sensitive release. Third, the introduction of HA-GA conjugate could improve active-targeting ability and uptake of cancer cells. The characteristics of the mixed micelles were determined by dynamic light scattering, ¹H NMR, transmission electron microscopy (TEM), and UV spectrophotometry. The in vitro cytotoxicity and cellular uptake of the mixed micelles were investigated in HepG2 and HeLa cells, and wound healing assays were performed to evaluate the effect of mixed micelles on cell migration. Furthermore, the in vivo antitumor efficacy of mixed micelles was evaluated in H22 tumor-bearing mice.

Materials and Methods

Materials

HA (MW: 210 kDa) was purchased from Freda Group (Jinan, China). DOX·HCl was obtained from Meilunbio (Dalian, China). GA was acquired from Fujie Pharmaceutical Co., Ltd. (China). 4-(4,6-Dimethoxy-1,3,5-triazin-2-yl)-4-methylmorpholinium chloride (DMT-MM) was purchased from Shanghai Medpep Co., Ltd. (China). Adipic acid dihydrazide (ADH) and 1-hydroxybenzotriazole (HOBt) were acquired from Shanghai Yuanye Biological Technology Co., Ltd. (China). DMEM medium, fetal bovine serum (FBS), 3-(4,5-dimethylthiazol-2-yl)-2,5-diphenyltetrazolium bromide (MTT), and 4',6-Diamidino-2-phenylindole (DAPI) were purchased from Beijing Solarbio Science & Technology Co., Ltd. (Beijing, China). Anti-CD31 antibody was obtained from Abcam (Shanghai, China). All other chemicals and reagents were of analytical grade.

Cell Culture

HepG2 and HeLa cells were obtained from Wuhan University Life Collection Center (Wuhan, China). HepG2 and HeLa cells were cultured in DMEM and RPMI 1640 medium with 10% fetal bovine serum (FBS) and 1% penicillin/streptomycin at 37°C in 5% CO₂ atmosphere.

Animals

Female BALB/c mice (age 7 weeks; weight approximately 20 g) were purchased from Pengyue Experimental Animal Breeding (Jinan, China). The animals were fed with

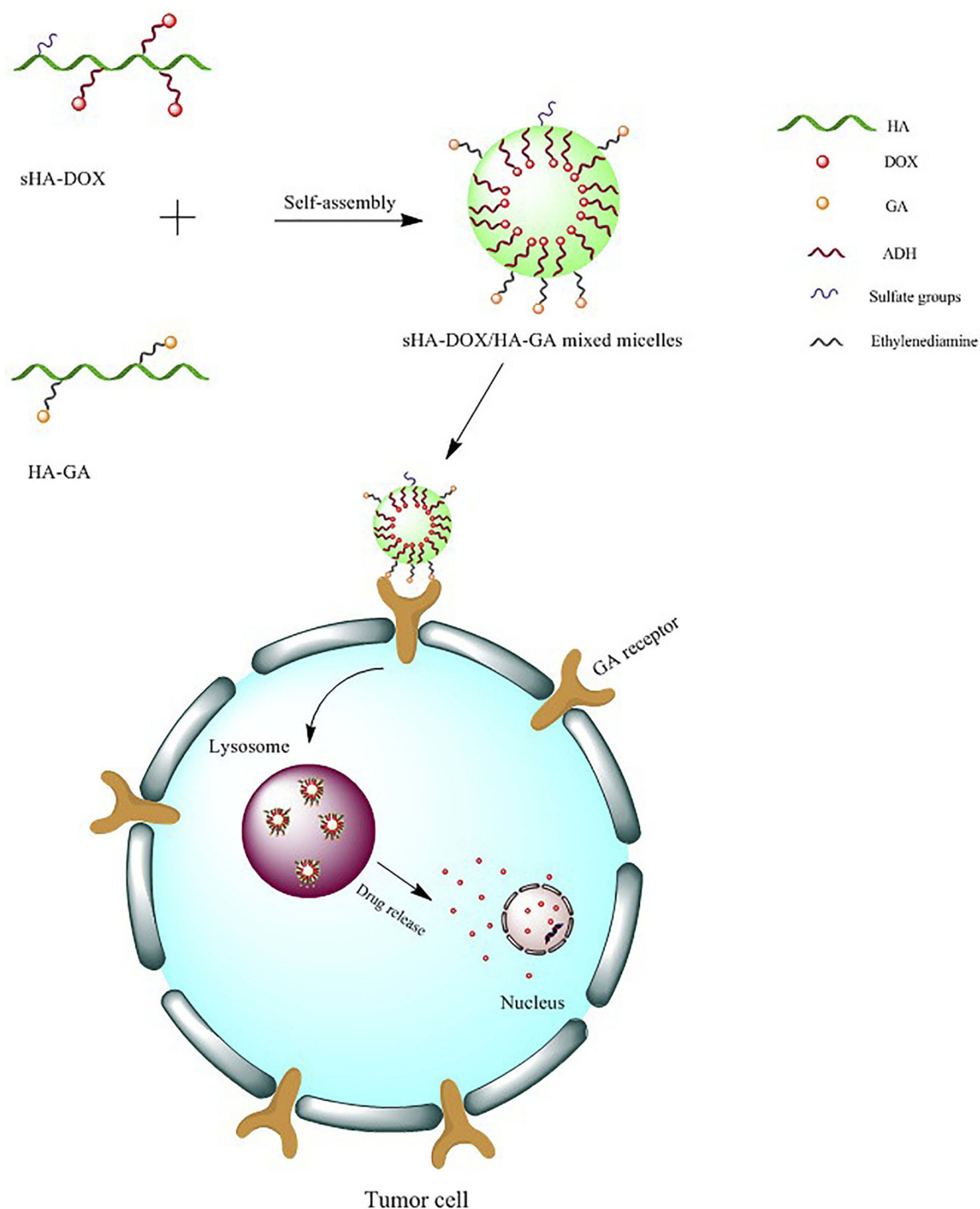


Figure 1 Illustration of the formation, uptake by tumor cells, and drug release of sHA-DOX/HA-GA mixed micelles.

Abbreviations: HA, hyaluronic acid; sHA, sulfated hyaluronic acid; DOX, doxorubicin; GA, glycyrrhethinic acid; ADH, adipic acid dihydrazide.

a standard diet and allowed water ad libitum. All animal experiments were carried out in compliance with the Animal Management Rules of the Ministry of Health of

the People's Republic of China (document number 55, 2001) and the Animal Experiment Ethics Review of Weifang Medical University (2017-025).

Preparation of sHA

sHA was synthesized as follows: First, 300 mg of HA were dissolved in 20 mL formylamine at 50°C. Second, HA was mixed with 15 mL chlorosulfonic acid–pyridine reagents (ratio of chlorosulfonic acid to pyridine was 1:4) at 60°C for 2 hrs. After the reaction, the pH value of the mixture solution was adjusted to 7.0 by the addition of 4 mol/L NaOH. Then, the reaction mixture was precipitated in excess ethanol, the precipitate was dissolved in water, and the result was dialyzed extensively against deionized water for 72 hrs and lyophilized. ¹H NMR and infrared spectroscopy (IR) were used to confirm the formation of sHA.

Synthesis of sHA-DOX and HA-GA Polymers

sHA-DOX was synthesized by a two-step reaction.³⁴ First, sHA-ADH was obtained by conjugating Adipic acid dihydrazide (ADH) to sHA through amide formation. Briefly, 100 mg of sHA were dissolved in 20 mL distilled water and then the carboxyl groups of sHA was activated by EDC and HOBt for 1 hr. Then, ADH was slowly added to the above solution. The reaction mixture was stirred for 24 hrs at room temperature, dialyzed against deionized water for 72 hrs, and lyophilized. Second, DOX and sHA-ADH were linked through an acid-labile hydrazone bond. In detail, 50 mg of sHA-ADH were dissolved in 10 mL of formylamine followed by the addition of DOX·HCl (10 mg) and TEA (10 µL). The reaction mixture was stirred at room temperature for 48 hrs under dark conditions. The resulting product of sHA-DOX was purified by dialysis against deionized water for 72 hrs and obtained after freeze-drying. HA-DOX was synthesized according to the above steps. The chemical structures of sHA and sHA-DOX were detected by ¹H NMR. To estimate the amount of conjugated DOX, 5 mg of sHA-DOX was dissolved in 1 mol/L HCl under stirring at room temperature for 24 hrs, and the amount of DOX was calculated using a UV spectrophotometer at the wavelength of 480 nm.

HA-GA was synthesized as previously described.³⁵ In brief, GA in methanol was activated with DMT-MM to form GA-ES. Then, GA-ES was slowly added to ethylene diamine solution to form GA-N. HA-GA was synthesized by coupling HA with GA-N through an amide bond in the presence of DMT-MM.

Preparation and Characterizations of sHA-DOX/HA-GA Mixed Micelles

sHA-DOX/HA-GA mixed micelles were prepared by an ultrasonic dispersion method. Briefly, both the sHA-DOX and HA-GA conjugates were dissolved in phosphate-buffered saline (PBS, pH 7.4) under gentle stirring at room temperature, and the mixture was ultrasonicated at 90 W for 15 mins under an ice bath by using a probe-type ultrasonicator (VCX-750, Sonics & Materials, Inc. Newtown, CT, USA). Additionally, sHA-DOX micelles and HA-GA micelles were also prepared under the same procedures.

The particle size and zeta potential of the different micelle formulations were measured by dynamic light scattering (Nano-ZS90, Malvern Zetasizer, UK), and the morphology of mixed micelles was visualized using TEM. Moreover, the critical micelle concentration (CMC) of sHA-DOX micelles was evaluated using fluorescence spectroscopy in the presence of pyrene molecules.²³

To evaluate the pH-responsive features of mixed micelles, sHA-DOX/HA-GA solution (1mg/mL) was incubated at pH 7.4, 6.8 and 5.5, and the particle sizes of mixed micelles were measured by dynamic light scattering at designated time intervals (0, 1, 2, 4, 6, and 8 hrs). In addition, the morphology of mixed micelles incubated at pH 5.5 for 4 hrs was visualized using TEM. To evaluate the stability of sHA-DOX/HA-GA mixed micelles, the particle size of mixed micelles in RPMI 1640 medium were measured for 7 days.

In vitro Release of DOX from Mixed Micelles

The DOX release from mixed micelles at different pH values was performed using the dialysis method. In brief, 3 mL solution of mixed micelles at the concentration of 1 mg/mL were transferred to a dialysis bag (MWCO=3500) and then immersed in 50 mL of PBS (pH 7.4, 6.8 and 5.5) containing 0.5% Tween 80. The release system was incubated at 37°C at 100 rpm under dark conditions. At designated time intervals (0.5, 1, 2, 4, 8, 12, 24, and 36 hrs), 4 mL of release medium were removed and replaced by 4 mL of fresh medium. The cumulative amounts of released DOX were calculated using a UV spectrophotometer at the wavelength of 480 nm.

In vitro Cytotoxicity Assay

The cytotoxicity of free DOX, HA-DOX, sHA-DOX, and sHA-DOX/HA-GA mixed micelles was assessed by MTT

assay against HepG2 and HeLa cells. Both HepG2 cells and HeLa cells were seeded into 96-well plates at a density of 5×10^3 cells per well and then cultured for 24 hrs at 37°C. Thereafter, the cells were treated with free DOX, HA-DOX, sHA-DOX, and sHA-DOX/HA-GA mixed micelles for 24 h at different concentrations of DOX (0.01–10 µg/mL). After incubation, 10 µL of MTT solution was added to each well and the cells were incubated for an additional 4 hrs. Then, the culture media were removed and 150 µL DMSO was added to each well. The absorbance at 490 nm was determined by a microplate reader (ELX800, Bio-Tek, Winooski, VT, USA).

Cellular Uptake

The cellular uptakes of sHA-DOX and sHA-DOX/HA-GA mixed micelles were determined by confocal laser scanning microscopy (CLSM).³⁶ In brief, HepG2 cells and HeLa cells were seeded on glass bottom cell culture dishes at a density of 1×10^4 cells/dish and then incubated for 24 hrs followed by the addition of sHA-DOX or sHA-DOX/HA-GA mixed micelles at a DOX concentration of 10 µg/mL, respectively. After incubation for 3 hrs, the media were removed and washed thrice with PBS. The cells were then fixed with 4% polyformaldehyde for 10 mins and dyed with DAPI for 10 mins. Subsequently, the cells were washed thrice with PBS and observed via confocal laser scanning microscopy (CLSM).

Cell Migration Assay

Cell migration inhibition was assessed using a wound healing assay.³¹ Briefly, the HepG2 cells were seeded into 6-well plates and incubated in a humidified 5% CO₂ atmosphere at 37°C. When the cells reached a confluence of 80% per well, the cells were streaked with a sterile pipette tip. After being washed thrice with PBS, the cells were treated with various formulations (DOX, HA-DOX, sHA, sHA-DOX, and sHA-DOX/HA-GA) and allowed 24 hrs to recover. Wound width was observed using a Nikon eclipse Ti-S microscope at 0 h and 24 hrs, and the cell migration rate was calculated.

In vivo Imaging Analysis

To observe the targeting properties of mixed micelles, DiR-loaded sHA-DOX/HA-GA mixed micelles were used to track the in vivo biodistribution of micelles. After the H22 tumor volume reached approximately 200 mm³, the BALB/c mice were randomly divided into two groups and injected intravenously via the tail vein

with DiR solution (as the control) or DiR-loaded sHA-DOX/HA-GA mixed micelles. The in vivo imaging system was used to analyze the in vivo biodistribution of micelles at 1, 3, 6, 12, 24 hrs after administration.

In vivo Antitumor Efficacy Study

Female BALB/c mice bearing H22 tumors were used to evaluate the antitumor efficacy of sHA-DOX/HA-GA mixed micelles. H22 cell suspensions (1×10^6 cells/0.1 mL) were implanted subcutaneously on the right flank of female BALB/c mice. When the tumor grew to approximately 150 mm³, the mice were randomly divided into five treatment groups (n=4 for each group): (1) normal saline (the control group), (2) free DOX, (3) HA-DOX, (4) sHA-DOX, (5) sHA-DOX/HA-GA mixed micelles. Various formulations were injected intravenously via the tail vein at DOX concentration of 3 mg/kg body weight, 7 times. The body weights and tumor volumes were measured every 2 days and calculated using the following equation: tumor volume (mm³) = $0.5 \times a \times b^2$, where a and b represent the longest and shortest tumor diameter, respectively. After 2 weeks' treatment, the mice were euthanatized. Tumors and the normal organ (heart) from each group were excised and fixed with 4% formaldehyde for further use.

Hematoxylin–Eosin (H&E) Staining and Immunohistochemistry Analysis

To further evaluate the antitumor efficacy of sHA-DOX/HA-GA mixed micelles, histological evaluation by hematoxylin–eosin (H&E) staining and immunohistochemistry analysis of microvessel density (MVD) assay were performed.^{37,38} In brief, 4% formaldehyde-fixed tumors and the normal organ (heart) from each group were embedded in paraffin blocks and then sections (4 µm thick) were cut using an ultrathin slicer. Afterwards, the tumor and heart sections were stained with hematoxylin (15 mins) and eosin (5 s) for histological evaluation. For microvessel density assay, a CD31 antibody was used to stain the tumor microvessels. Images of tumor microvessels were taken using fluorescence microscopy (Olympus IX51, Japan).

Statistical Analysis

All experimental data were expressed as mean ± standard deviation (SD). Statistical significance was tested using a Student's *t*-test, and *P*<0.05 indicated statistical significance.

Results and Discussion

Synthesis of sHA-DOX Polymers

The procedure for synthesizing sHA-DOX polymers is shown in Figure 2. sHA was synthesized by adding chlorosulfonic acid–pyridine to HA, and sHA-DOX polymers were obtained by conjugating DOX to sHA via an acid-labile hydrazone bond. The structure of sHA-DOX polymers was confirmed by IR and ^1H NMR (Figure 3). As shown in Figure 3A, the absorption bands at 3200–3600 cm^{-1} belong to the $-\text{OH}$ group of HA, and the band at 830 cm^{-1} was attributed to the $\text{C}-\text{O}-\text{S}$ stretching vibration. The characteristic band at 830 cm^{-1} was confirmed in sHA and sHA-DOX polymers, indicating that the $-\text{SO}_3\text{H}$ group was successfully introduced into HA polymers. Furthermore, the ^1H NMR spectra of HA, sHA, DOX, and sHA-DOX polymers were shown in Figure 3B. The peak appearing at 2.0 ppm ($-\text{NOCH}_3$) was attributed to methyl groups of HA; the characteristic peaks at 7.8–7.2 ppm were assigned to the protons of the aromatic benzene ring in DOX. In the spectra of sHA-DOX polymers, new characteristic peaks appeared at 7.8–7.2 ppm (DOX), indicating that DOX was successfully grafted to sHA. Additionally, the content of conjugated DOX was determined to be 14.42% using UV detection.

Preparation and Characterization of sHA-DOX/HA-GA Mixed Micelles

sHA-DOX/HA-GA polymers were self-assembled into micellar structures in aqueous solution with HA as hydrophilic shells and DOX as hydrophobic cores (Figure 1). As shown in Table 1, the particle sizes of sHA-DOX micelles, HA-GA micelles, and sHA-DOX/HA-GA mixed micelles were 230.83 ± 3.40 , 183.37 ± 2.48 , and 217.70 ± 0.89 nm, respectively (Figure 4A–C). Compared to sHA-DOX micelles, the particle size of mixed micelles decreased due to the hydrophobic GA group increasing the hydrophobic cohesion of mixed micelles. On the other hand, the zeta potentials of sHA-DOX micelles, HA-GA micelles, and sHA-DOX/HA-GA mixed micelles were -30.13 ± 3.53 , -34.60 ± 0.46 and -31.87 ± 0.61 mV, respectively. All the mixed micelles showed negative zeta potential values, which play an important role in minimizing plasma protein adsorption and nonspecific cellular uptake.³⁹ Moreover, the stability of mixed micelles was determined for 2 weeks in PBS, and there were no significant changes in particle size and zeta potential (Figure 4D and E). Additionally, no obvious particle size changes were observed in RPMI 1640 medium for 7 days (Figure 4F).

This result indicated that the mixed micelles are highly stable. Additionally, TEM was used to visualize the morphologies of mixed micelles. The TEM images in Figure 5B revealed that the mixed micelles were spherical in shape. Furthermore, the critical micelle concentration (CMC) of sHA-DOX conjugates was 38.02 $\mu\text{g/mL}$, which indicated that the low CMC values might have resistance to dissociation at highly diluted conditions in the body (Supporting Figure 1).

pH-Responsive Behaviors of sHA-DOX/HA-GA Mixed Micelles

The pH-response behaviors of sHA-DOX/HA-GA were evaluated under different pH conditions (pH 7.4, 6.8, and 5.5). As shown in Figure 5A, the particle size of sHA-DOX/HA-GA increased significantly within 8 hrs at pH 5.5. However, the mixed micelles could maintain stability at pH 7.4. This result suggested that the hydrazone bonds in mixed micelles could be cleaved under acidic conditions, leading to the disintegration of micelles. The pH-response behavior of the mixed micelles was also confirmed by TEM. As shown in Figure 5C, after incubation at pH 5.5 for 4 hrs, the mixed micelles became irregular and broken in shape. These results demonstrated that the pH-responsive behaviors of mixed micelles may be triggered at low pH value due to the acid-sensitive cleavage of the hydrazone bond.

In vitro DOX Release from the sHA-DOX/HA-GA Mixed Micelles

DOX was conjugated to sHA segment through an acid-labile hydrazone bond. The in vitro drug release was evaluated at pH values of 7.4, 6.8, and 5.5. As shown in Figure 6, DOX showed pH-responsive release from the mixed micelles within 36 hrs. At pH 5.5, its cumulative release rate was 91.95%, significantly higher than at pH 6.8 (69.34%) and pH 7.4 (58.47%). The results suggested that the cleavage of the hydrazone bond in mixed micelles occurred rapidly at pH 5.5, indicating that DOX might be released from the mixed micelles in lysosomes (pH 5.0–6.0).⁶ The results showed that the mixed micelles were stable under physiological condition (pH 7.4), but could release drugs in acidic lysosomal conditions, resulting in higher bioavailability than just the free drug.

In vitro Cellular Uptake

The cellular uptake of sHA-DOX and sHA-DOX/HA-GA mixed micelles were evaluated in HepG2 and HeLa cells

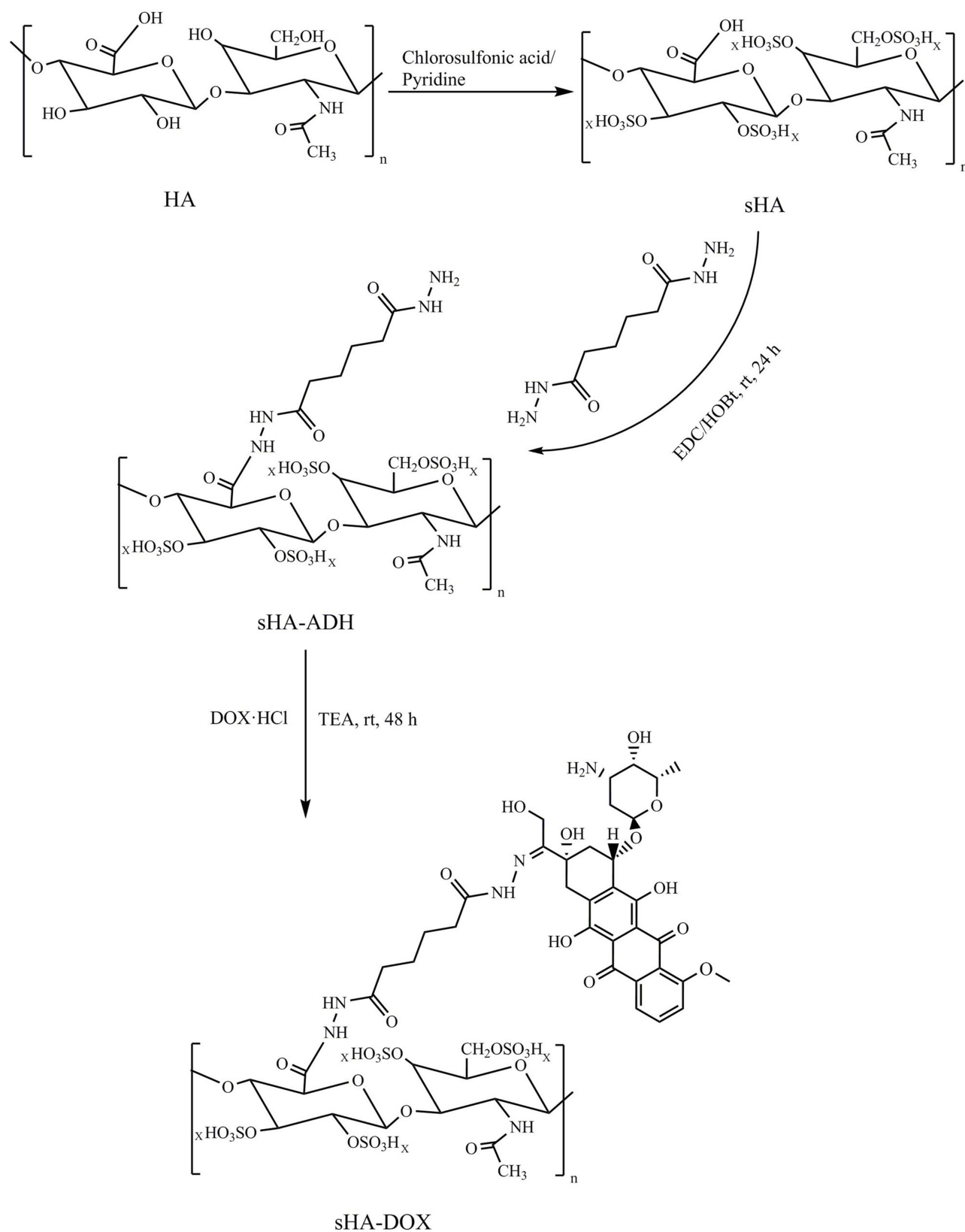


Figure 2 Synthesis of sHA-DOX Polymers.

Note: $0 < x \leq 1$, otherwise $-\text{OH}$ group.

Abbreviations: HA, hyaluronic acid; sHA, sulfated hyaluronic acid; HOBt, 1-hydroxybenzotriazole; EDC, 1-(3-dimethylaminopropyl)-3-ethylcarbodiimide hydrochloride; DOX·HCl, doxorubicin HCl; DOX, doxorubicin; TEA, triethylamine; rt, room temperature.

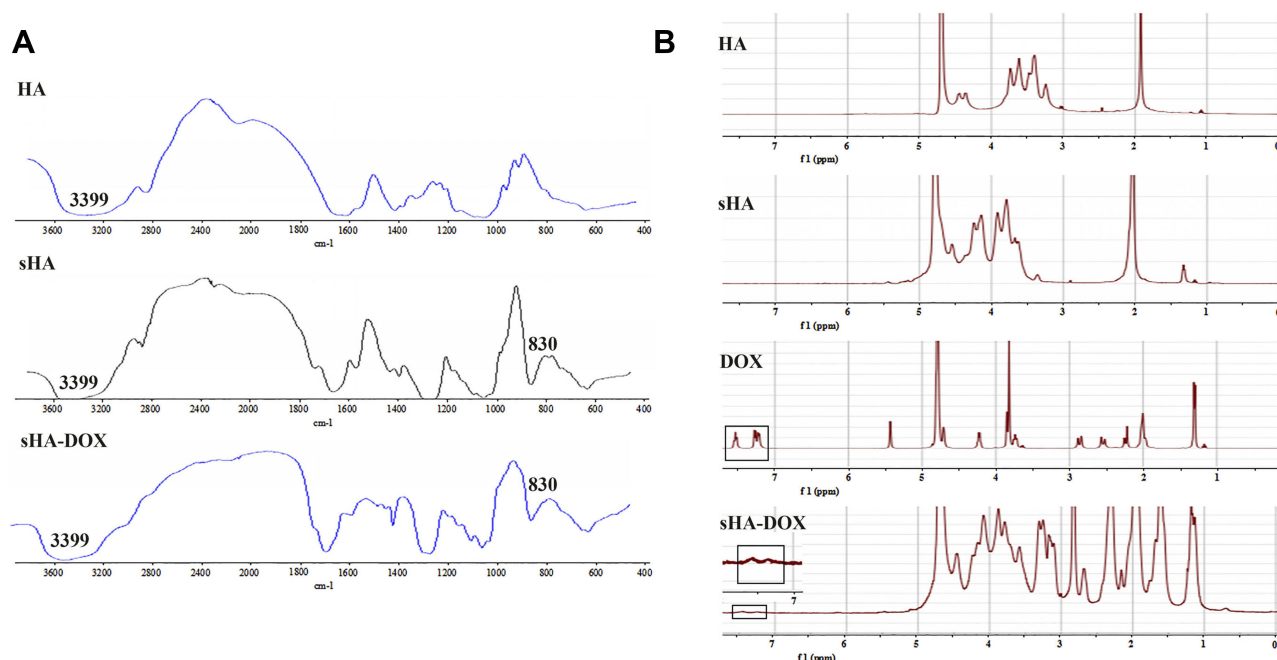


Figure 3 (A) IR spectra of HA, sHA and sHA-DOX Polymers, (B) ¹H NMR spectra of HA, sHA, DOX and sHA-DOX Polymers in D₂O.

Abbreviations: HA, hyaluronic acid; sHA, sulfated hyaluronic acid; DOX, doxorubicin; IR, infrared spectroscopy; NMR, nuclear magnetic resonance.

Table 1 Characterization of Different Micelles

	DLS (nm)	PDI	ζ-Potential (mV)
sHA-DOX	230.83±3.40	0.02±0.01	-30.13±3.53
HA-GA	183.37±2.48	0.21±0.02	-34.60±0.46
sHA-DOX/HA-GA	217.70±0.89	0.07±0.04	-31.87±0.61

Note: Data represent mean ± SD.

Abbreviations: HA, hyaluronic acid; sHA, sulfated hyaluronic acid; DOX, doxorubicin; GA, glycyrrhetic acid; DLS, dynamic light scattering; PDI, polydispersity index.

using CLSM. As shown in Figure 7, DOX (red fluorescence) was used to track the micelles, and cell nuclei were located using DAPI (blue fluorescence). After incubation with the micelles for 3 hrs, the red fluorescence of DOX could be detected in tumor cells. This result indicated that the micelles could be easily taken up by tumor cells. As shown in Figure 7A and B, sHA-DOX/HA-GA mixed micelles showed stronger red fluorescence than sHA-DOX in liver carcinoma cells, suggesting that the introduction of GA group in mixed micelles promoted liver-targeting delivery of anti-cancer drugs. However, there was no significant difference in red fluorescence intensity between sHA-DOX and sHA-DOX/HA-GA treatment in HeLa cells (Figure 7C and D). This might be due to the fact that the GA-receptor was not expressed in HeLa cells, and the addition of GA-HA conjugates in mixed micelles did not affect the DOX uptake by HeLa cells. Based on the

above results, it could be concluded that the presence of GA in mixed micelles could enhance the cellular uptake of micelles in liver cancer cells via GA-receptor-mediated endocytosis.^{40,41} Overall, these results suggested that the mixed micelles have the potential to deliver chemotherapy drugs for anti-hepatoma therapy.

In vitro Cytotoxicity Assay

The cytotoxicities of free DOX, HA-DOX, sHA-DOX, and sHA-DOX/HA-GA in HepG2 and HeLa cells were evaluated by MTT assay. As shown in Figure 8A and B, all the formulations showed concentration-dependent cytotoxicities in both HepG2 and HeLa cells. Compared to free DOX and HA-DOX formulations, two other micelles based on sHA-DOX polymers exhibited higher cytotoxicity. A possible explanation is that sHA could inhibit tumor migration, thereby improving the cytotoxicity of DOX through a synergistic effect. Interestingly, the cytotoxicity of sHA-DOX/HA-GA mixed micelles on HepG2 cells was stronger than that of sHA-DOX micelles, but there were no significant differences between the two formulations on HeLa cells. This might be because the GA-HA conjugate in mixed micelles increased DOX uptake via GA-receptor-mediated endocytosis in HepG2 cells with high GA-receptor expression, but had no effect on HeLa cells without GA-receptor expression.⁴²

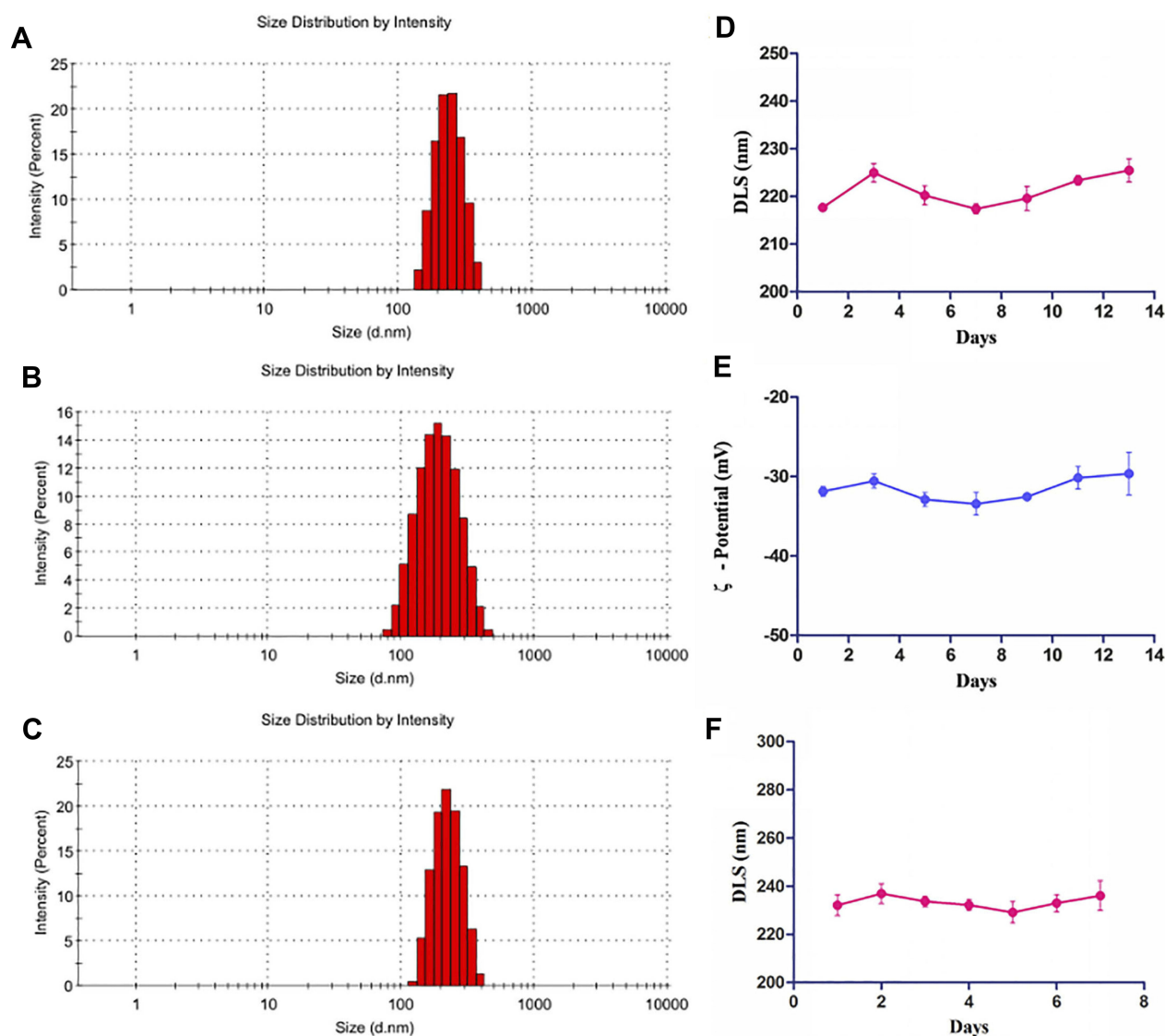


Figure 4 The stability of sHA-DOX/HA-GA mixed micelles.

Notes: The particle size distribution of sHA-DOX (**A**), HA-GA (**B**), sHA-DOX/HA-GA (**C**); the particle size (**D**) and zeta potential (**E**) of sHA-DOX/HA-GA mixed micelles for 2 weeks in PBS; the particle size changes of sHA-DOX/HA-GA mixed micelles for 7 days in RPMI 1640 medium (**F**).

Abbreviations: HA, hyaluronic acid; sHA, sulfated hyaluronic acid; DOX, doxorubicin; GA, glycyrrhetinic acid; DLS, dynamic light scattering.

Cell Migration Assay

To evaluate the cell migration ability of DOX, HA-DOX, sHA, sHA-DOX, and sHA-DOX/HA-GA, a wound healing assay was performed with serum-free medium as control. Cell motility to the denuded area was measured by ImageJ after 24 hrs. As shown in [Figure 9A and B](#), cells treated with serum-free medium showed high cell migration ability. Compared to the control group, the five drug formulations exhibited inhibition of cell migration. Interestingly, sHA was a more effective inhibitor of cell migration than DOX or HA-DOX, suggesting that HAase plays an important role in cellular growth and migration

and that the sHA conjugate might restrict the motility of tumor cells by inhibiting HAase activity.^{18–21} In addition, sHA-DOX showed stronger inhibition of tumor cell migration than sHA. The possible explanation was that sHA-DOX might block the motility of tumor cells through combined effects of sHA-inhibiting HAase activity and DOX-induced apoptosis. Furthermore, sHA-DOX/HA-GA mixed micelles were most effective in inhibiting cell migration with a migration rate of only 3.38%, and this result was consistent with the cytotoxicity result, in which the mixed micelles exhibited the highest cytotoxicity among all the formulations. The GA molecule in mixed

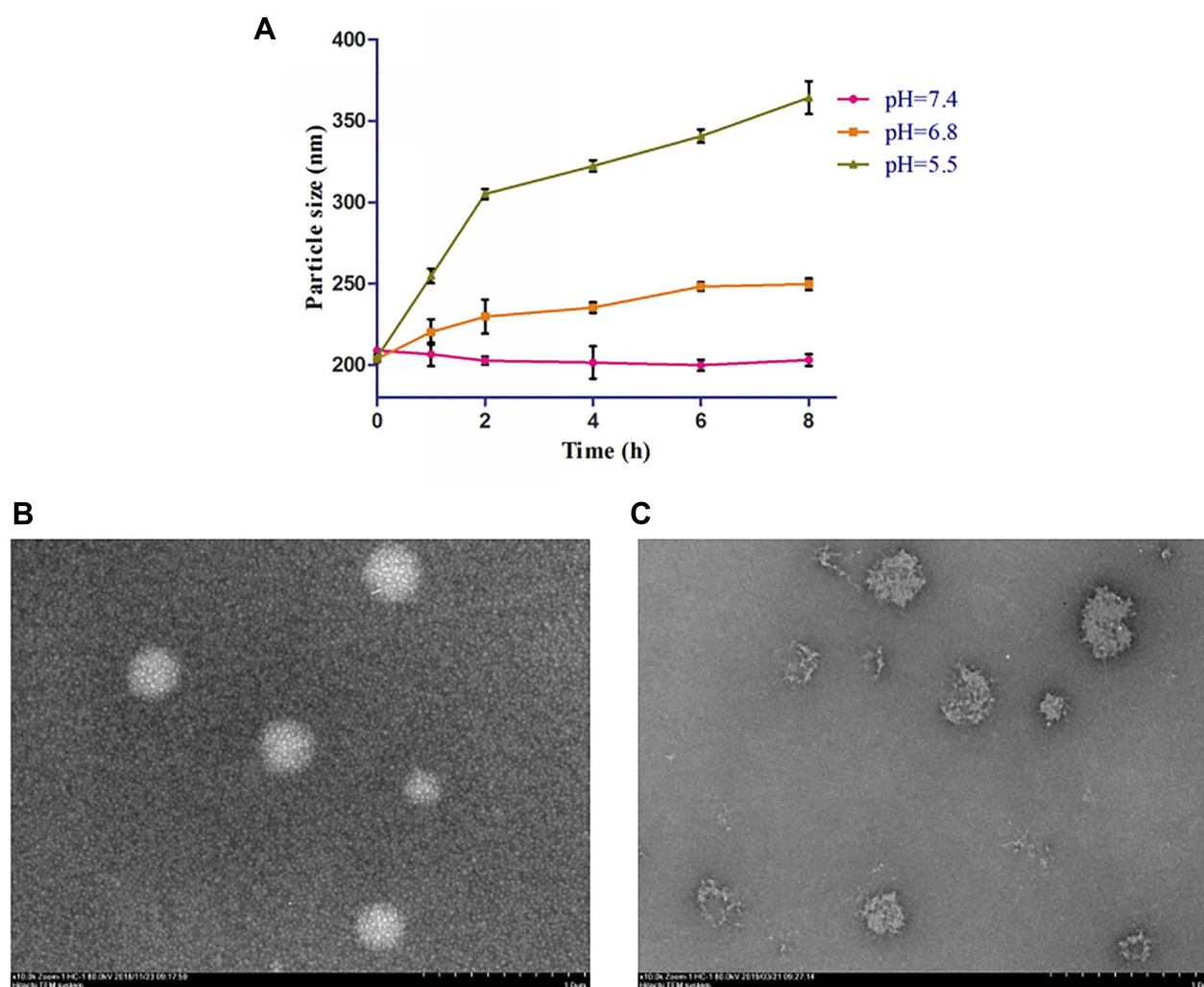


Figure 5 pH-responsive size behaviors of mixed micelles.

Notes: (A) Particle size variation of mixed micelles at different pH values within 8 hrs. (B) TEM image of mixed micelles at pH 7.4. (C) TEM image of mixed micelles at pH 5.5 after 4 hrs.

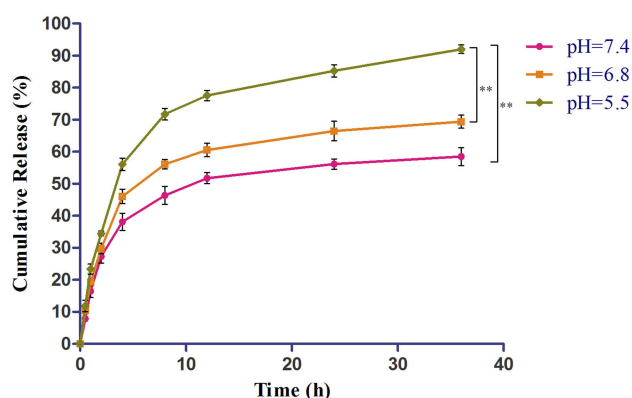


Figure 6 In vitro release of DOX from sHA-DOX/HA-GA mixed micelles.

Notes: Release medium: 50 mL of PBS (pH 7.4, 6.8, and 5.5) containing 0.5% Tween 80; Release condition: 37°C, 100 rpm, under dark condition. **P<0.01. **Abbreviations:** HA, hyaluronic acid; sHA, sulfated hyaluronic acid; DOX, doxorubicin; GA, glycyrrhetic acid.

micelles might contribute to cellular uptake, resulting in a stronger inhibition effect on tumor cell migration.

In vivo Biodistribution of sHA-DOX/HA-GA Mixed Micelles

The in vivo biodistribution and tumor-targeting properties of mixed micelles were evaluated using a real-time NIRF imaging technique. As shown in Figure 10A and B, the NIRF signals in the tumor region for the free DiR were lower than that for the DiR-loaded sHA-DOX/HA-GA mixed micelles, which indicates that the enhanced tumor accumulation of DiR might be attributable to the GA molecule in mixed micelles, and suggests that the GA molecule improved the active targeting ability of mixed micelles.

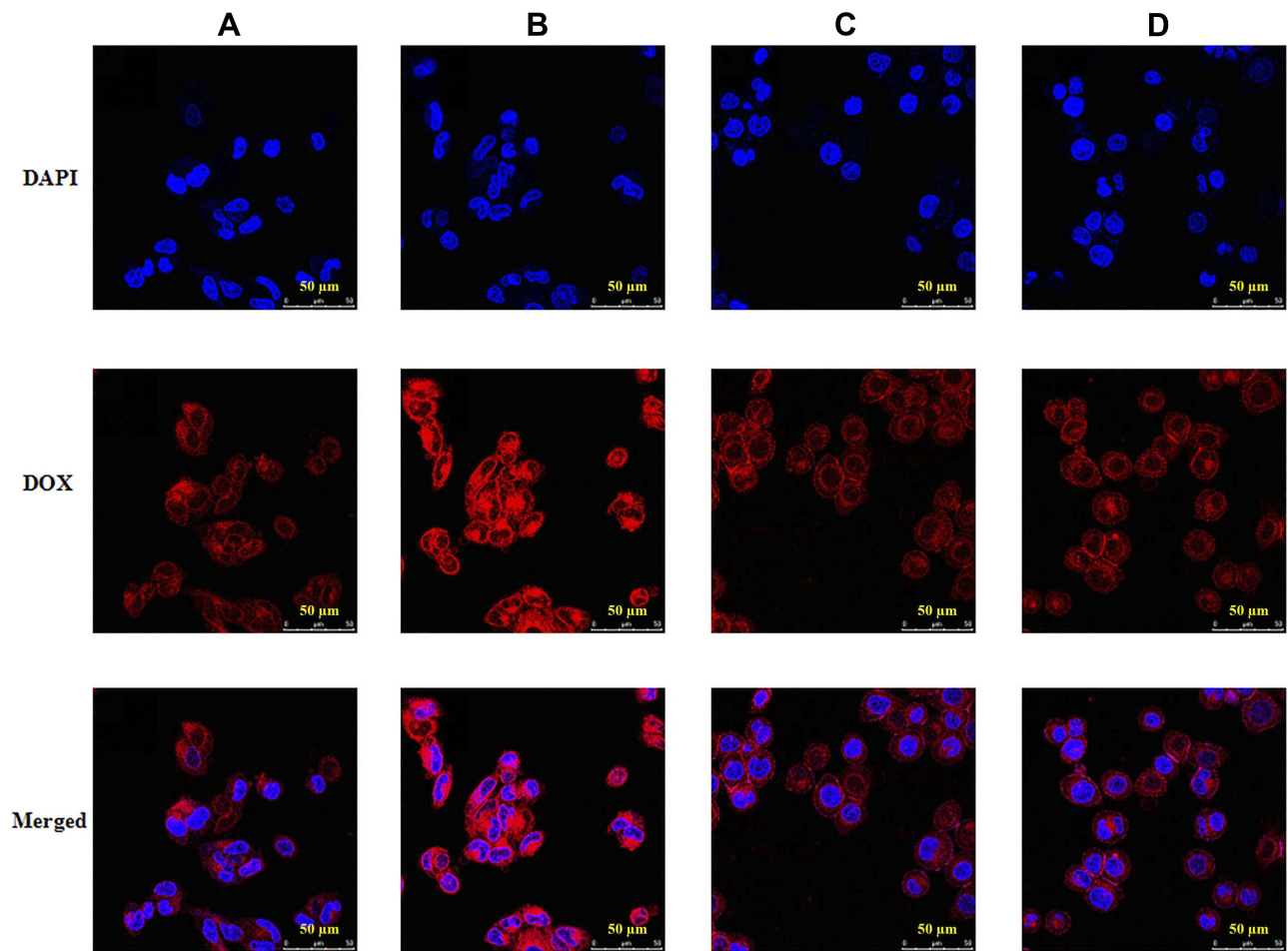


Figure 7 Confocal images of HepG2 cells incubated with sHA-DOX (A) and sHA-DOX/HA-GA (B); HeLa cells incubated with sHA-DOX (C) and sHA-DOX/HA-GA (D). **Note:** DAPI (blue), DOX (red) and a merge of two images were simultaneously presented.

Abbreviations: HA, hyaluronic acid; sHA, sulfated hyaluronic acid; DAPI, 4',6-diamidino-2-phenylindole; DOX, doxorubicin; GA, glycyrrhetic acid.

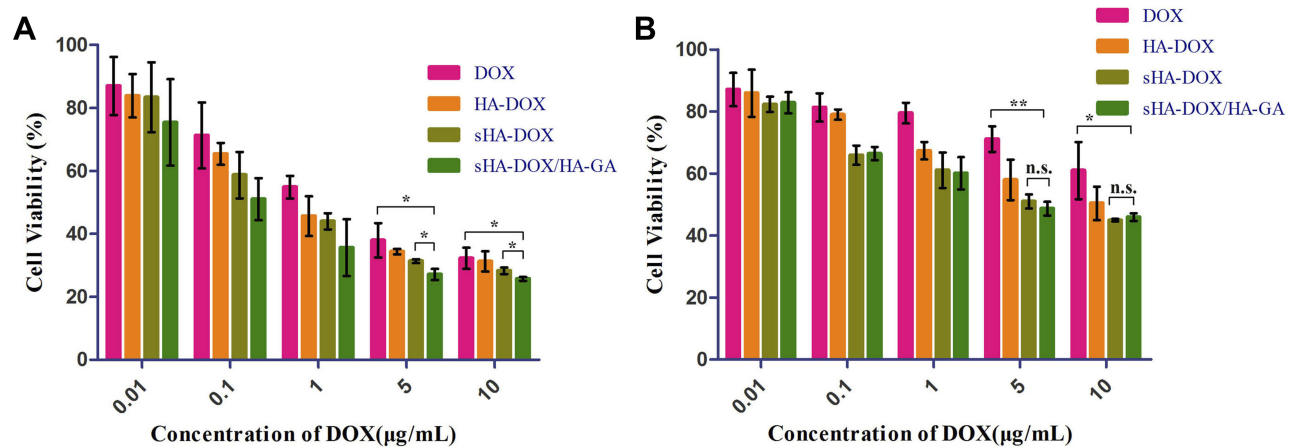


Figure 8 Cytotoxicity of HepG2 (A) and HeLa cells (B) incubated with different concentrations of free DOX, HA-DOX, sHA-DOX and sHA-DOX/HA-GA for 24 hrs.

Notes: * $P < 0.05$, free DOX vs sHA-DOX/HA-GA group, sHA-DOX vs sHA-DOX/HA-GA group; ** $P < 0.01$, free DOX vs sHA-DOX/HA-GA group; n.s., nonsignificant.

Abbreviations: HA, hyaluronic acid; sHA, sulfated hyaluronic acid; DOX, doxorubicin; GA, glycyrrhetic acid.

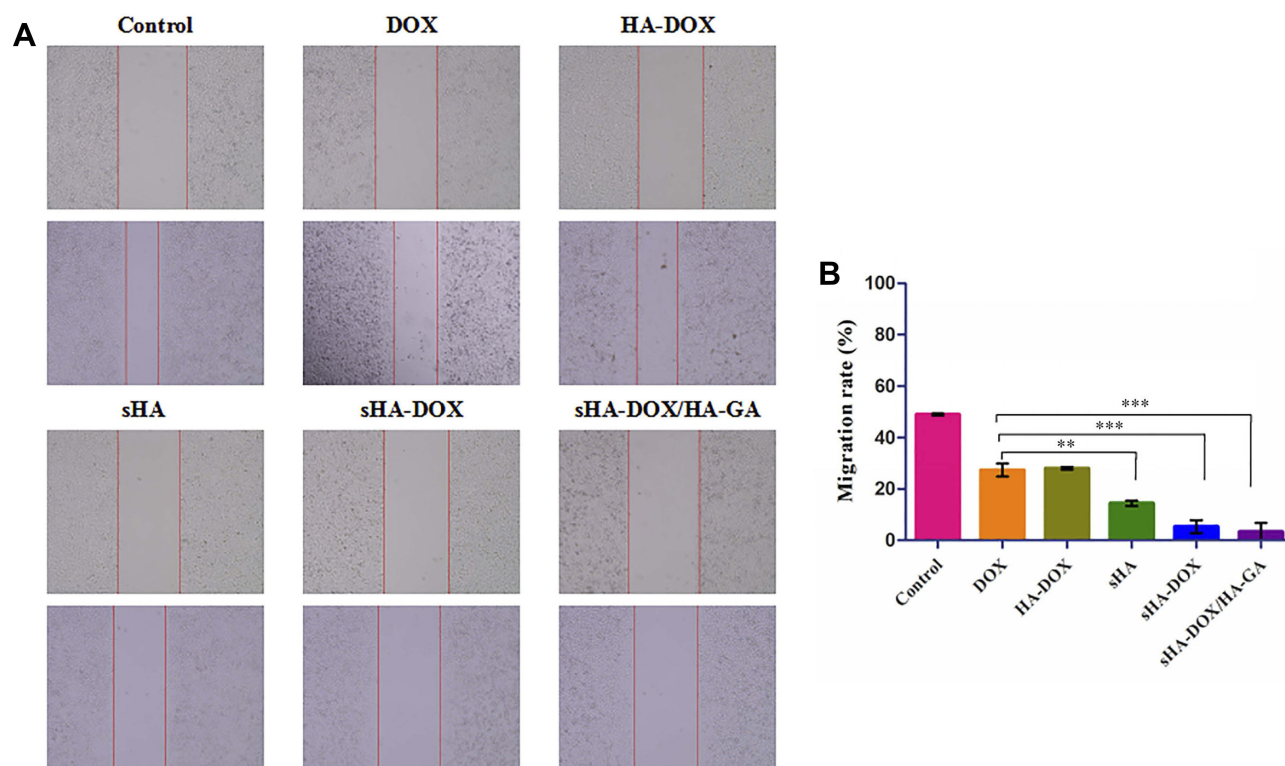
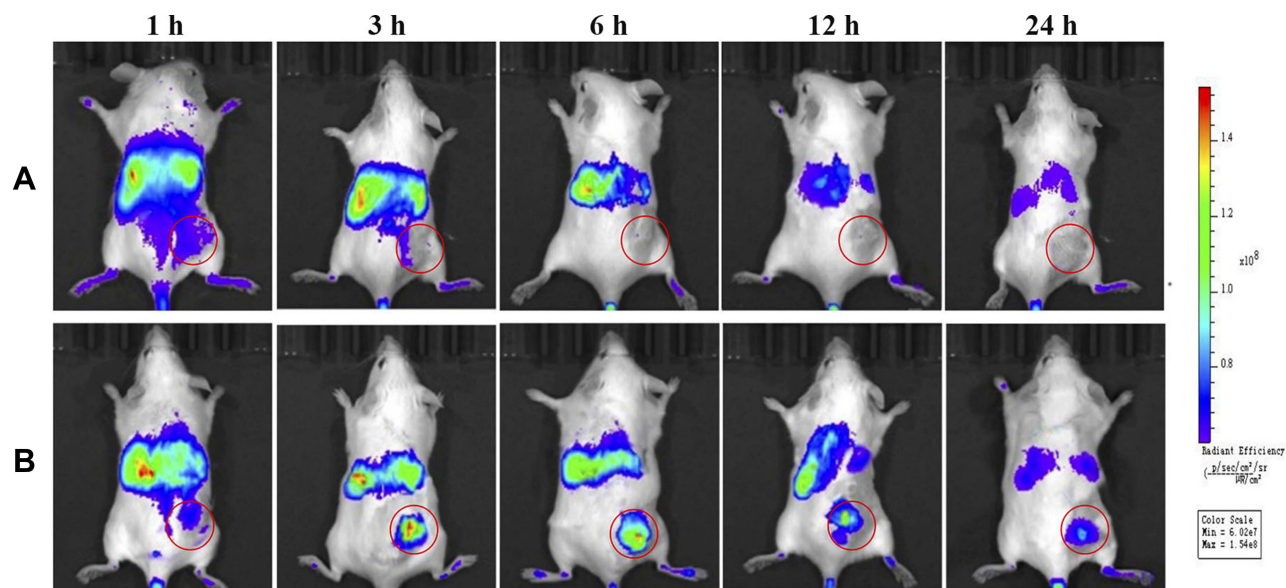


Figure 9 Effect of DOX, HA-DOX, sHA, sHA-DOX, and sHA-DOX/HA-GA on cell migration (A). Cell migration rate from 0 to 24 hrs was calculated by ImageJ (B). **Notes:** Data represent mean \pm SD (n=3); Control cells treated with serum-free medium. **P<0.01, statistically significant difference between free DOX and sHA group; ***P<0.001, statistically significant difference between free DOX and sHA-DOX group, between free DOX and sHA-DOX/HA-GA group. **Abbreviations:** HA, hyaluronic acid; sHA, sulfated hyaluronic acid; DOX, doxorubicin; GA, glycyrrhethinic acid.



In vivo Antitumor Efficacy Study

The antitumor effect of various formulations on H22 tumor-bearing mice was shown in Figure 11. After 2 weeks of treatment, the body weight of the free DOX group was lower than that of the saline group, and there was no significant difference between the micelles groups and the saline group (Figure 11A). The results suggested that these micelle formulations had better biocompatibility than free DOX. The tumor growth curves and the images of excised tumors were shown in Figure 11B and C. The tumor volume of mice treated with normal saline increased rapidly, and the groups treated by drug formulations showed obvious inhibition of tumor growth. Compared to free DOX, all of the micelle formulations exhibited higher anti-tumor effect. The results might be

due to the fact that nano-delivery systems could promote the accumulation of DOX in tumor regions via the enhanced permeability and retention (EPR) effect.⁴³ As expected, the average tumor volume of the sHA-DOX group was $344 \pm 68 \text{ mm}^3$, which was significantly lower than that of the HA-DOX group ($683 \pm 146 \text{ mm}^3$), suggesting that sulphation modification on the HA chain promoted the anti-tumor effect by inhibiting tumor migration. Furthermore, the sHA-DOX/HA-GA-treated group showed superior tumor inhibition compared with other drug formulation groups. This may be due to the fact that the mixed micelles could be taken up by tumor cells via liver-targeting delivery and effectively release DOX in tumor cells owing to pH-sensitive hydrolysis, resulting in an admirable antitumor effect.

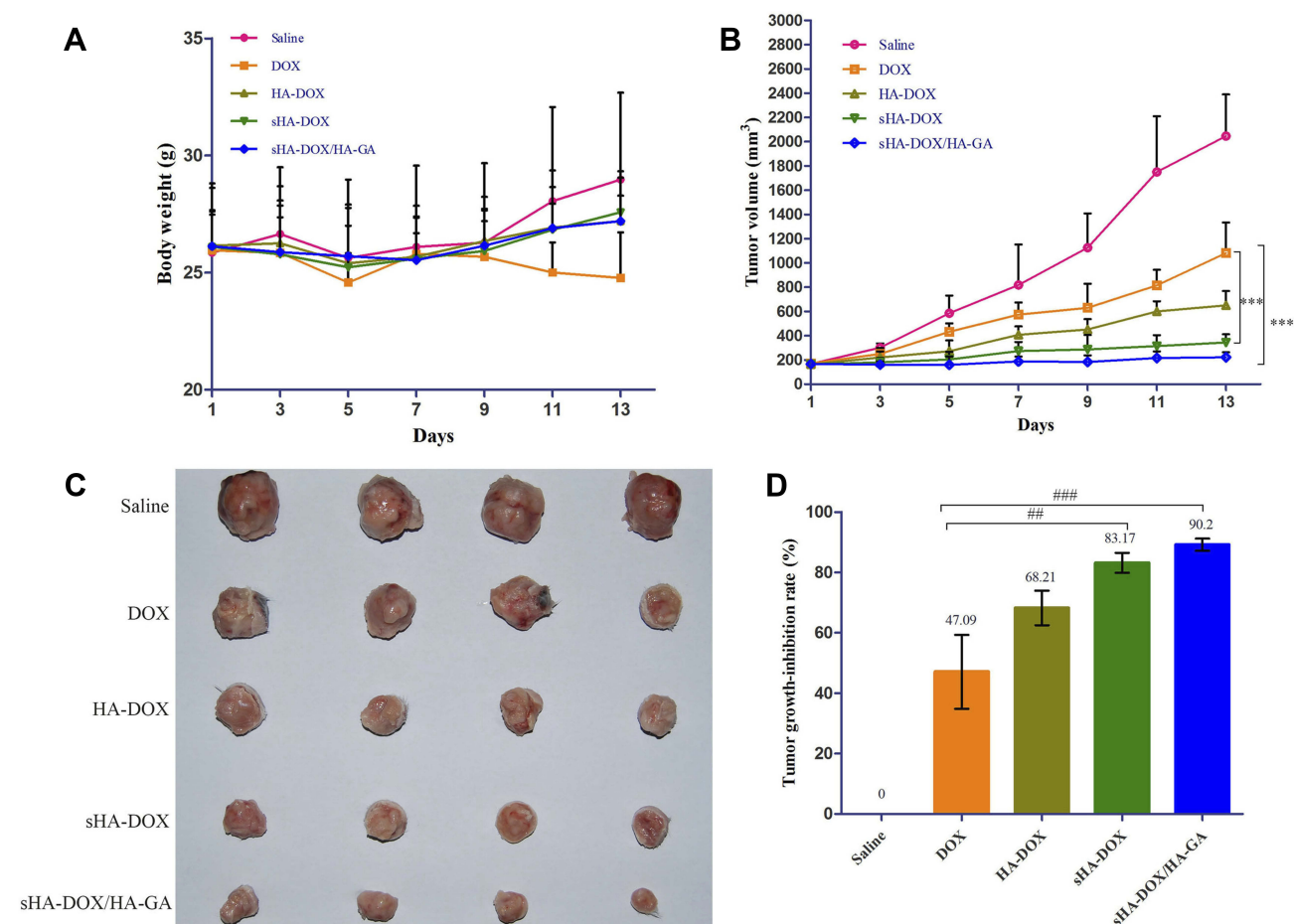


Figure 11 In vivo antitumor efficacy of DOX, HA-DOX, sHA-DOX, and sHA-DOX/HA-GA on H22 tumor-bearing mice. (A) The changes in body weight of female BALB/c mice; (B) Tumor growth curve; (C) The images of excised tumors; (D) Tumor growth-inhibition rate. The error bars represent standard deviation (n=4).

Notes: Saline, mice treated with normal saline via tail vein injection. ***P<0.001, statistically significant difference between free DOX and sHA-DOX group, between free DOX and sHA-DOX/HA-GA group; ##P<0.01, statistically significant difference between free DOX and sHA-DOX group; ####P<0.001, statistically significant difference between free DOX and sHA-DOX/HA-GA group.

Abbreviations: HA, hyaluronic acid; sHA, sulfated hyaluronic acid; DOX, doxorubicin; GA, glycyrrhetic acid.

H&E Staining and Immunohistochemistry Analysis

H&E staining and MVD assay were performed to evaluate the antitumor efficacy of sHA-DOX/HA-GA mixed micelles. As shown in Figure 12A, no significant tumor necrosis was observed in the saline group. By contrast, obvious karyolysis and cytoplasmic vacuolation appeared in different drug formulation groups. In addition, the necrotic area of the sHA-DOX group was significantly larger than that of the HA-DOX group, indicating that sHA-DOX had a stronger tumor inhibition effect. The results were consistent with their anti-tumor efficacy in vivo. Furthermore, compared to sHA-DOX, sHA-DOX/HA-GA mixed micelles induced more shrunken nuclei and lower cellular density, indicating that the micelles modified by GA group could exert a better antitumor effect than GA-free micelles.

In vivo organ toxicity evaluation is important for the clinical application of drug delivery systems.⁴⁴ Heart damage is an essential indicator to assess DOX-induced organ toxicity. As shown in Figure 12B, mice treated with free DOX showed obvious intercellular vacuolation of myocardial fibers, while no significant heart damage was observed in HA-DOX, sHA-DOX, and sHA-DOX/HA-

GA treatment groups. This result indicated that intelligent drug delivery system could significantly reduce the systemic toxicity of DOX.

The tumor growth, metastasis, and invasion are associated with angiogenesis. For MVD assay, the expression of CD31-positive tumor microvessels (brown areas) is shown in Figure 12C. The MVD assay showed that there were fewer tumor microvessels in the sHA-DOX group than in the HA-DOX group, suggesting that sHA also inhibited tumor angiogenesis. Moreover, the sHA-DOX/HA-GA treatment group showed the fewest tumor microvessels, indicating its excellent antitumor effect.

Conclusion

pH-sensitive and hepatoma-targeting mixed micelles consisting of sHA-DOX conjugates and HA-GA conjugates were prepared in the study. The mixed micelles were spherical in shape and showed the pH-responsive release of DOX at acidic conditions. Moreover, the mixed micelles could effectively deliver DOX into HepG2 cells, inhibit tumor migration, and exhibit higher anti-tumor efficacy than free DOX in vitro and in vivo. In conclusion, sHA-DOX/HA-GA mixed micelles could be a promising intelligent drug delivery system for anti-hepatoma therapy.

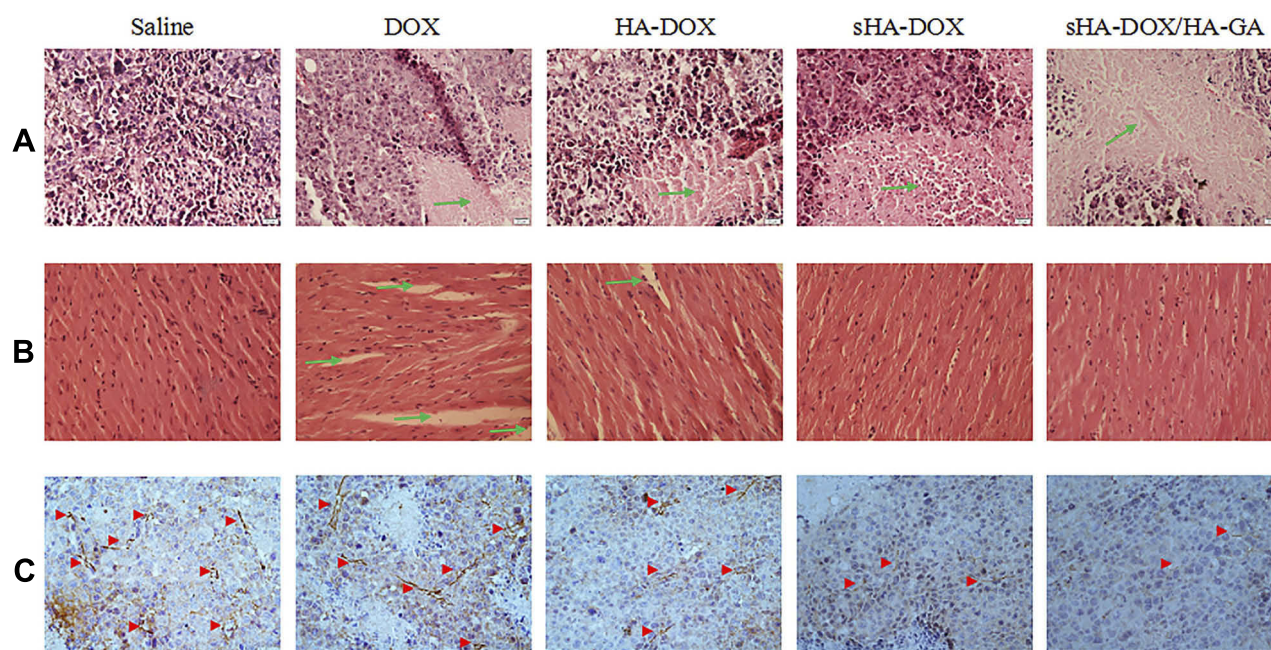


Figure 12 Images of H&E assays for tumors (A), hearts (B), and MVD determination by immunohistochemistry on formaldehyde-fixed tumors (C) after treatment with saline, free DOX, HA-DOX, sHA-DOX and sHA-DOX/HA-GA for 2 weeks. For all images, magnification is 400 ×.

Notes: Saline, mice treated with normal saline via tail vein injection. Green arrows indicate tumor necrotic area in (A), myocardial injury area in (B). Red arrowheads indicate the tumor microvessels in (C).

Abbreviations: HA, hyaluronic acid; sHA, sulfated hyaluronic acid; DOX, doxorubicin; GA, glycyrrhetic acid; H&E, Hematoxylin-eosin; MVD, microvessel density.

Acknowledgments

This work was supported by the National Science Foundation of China (81803464), Natural Science Foundation of Shandong Province (ZR2018BH041), the Education Science and Technology Project of Shandong Province (J17KA141), Medical and Health Technology Development Program in Shandong Province (2016WS0673), and Project of Traditional Chinese Medicine Technology Development Program in Shandong Province (2017-212).

Disclosure

The authors report no conflicts of interest in this work.

References

- Manieri E, Herrera-Melle L, Mora A, et al. Adiponectin accounts for gender differences in hepatocellular carcinoma incidence. *J Exp Med*. 2019;216(5):1108–1119. doi:10.1084/jem.20181288
- Bray F, Ferlay J, Soerjomataram I, et al. Global cancer statistics 2018: GLOBOCAN estimates of incidence and mortality worldwide for 36 cancers in 185 countries. *CA Cancer J Clin*. 2018;68(6):394–424. doi:10.3322/caac.v68.6
- Sia D, Villanueva A, Friedman SL. Liver cancer cell of origin, molecular class, and effects on patient prognosis. *Gastroenterology*. 2017;152(4):745–761. doi:10.1053/j.gastro.2016.11.048
- Gravitz L. Liver cancer. *Nature*. 2014;516(7529):S1. doi:10.1038/516S1a
- Yin T, Wang L, Yin L, et al. Co-delivery of hydrophobic paclitaxel and hydrophilic AURKA specific siRNA by redox-sensitive micelles for effective treatment of breast cancer. *Biomaterials*. 2015;61:10–25. doi:10.1016/j.biomaterials.2015.05.022
- Ma B, Zhuang W, Wang Y, et al. pH-sensitive doxorubicin-conjugated prodrug micelles with charge-conversion for cancer therapy. *Acta Biomater*. 2018;70:186–196. doi:10.1016/j.actbio.2018.02.008
- Bae KH, Tan S, Yamashita A, et al. Hyaluronic acid-green tea catechin micellar nanocomplexes: fail-safe cisplatin nanomedicine for the treatment of ovarian cancer without off-target toxicity. *Biomaterials*. 2017;148:41–53. doi:10.1016/j.biomaterials.2017.09.027
- Wang Y, Wang F, Liu Y, et al. Glutathione deionated and pH responsive nano-clusters of Au nanorods with a high dose of DOX for treatment of multidrug resistant cancer. *Acta Biomater*. 2018;75:334–345. doi:10.1016/j.actbio.2018.06.012
- Kesharwani SS, Kaur S, Tummala H. Overcoming multiple drug resistance in cancer using polymeric micelles. *Expert Opin Drug Deliv*. 2018;15(11):1127–1142. doi:10.1080/17425247.2018.1537261
- Kesharwani SS, Kaur S, Tummala H. Multifunctional approaches utilizing polymeric micelles to circumvent multidrug resistant tumors. *Colloids Surf B Biointerfaces*. 2019;173:581–590. doi:10.1016/j.colsurfb.2018.10.022
- Zhu C, Zhang H, Li W, et al. Suppress orthotopic colon cancer and its metastasis through exact targeting and highly selective drug release by a smart nanomicelle. *Biomaterials*. 2018;161:144–153. doi:10.1016/j.biomaterials.2018.01.043
- Chen Z, He N, Chen M, et al. Tunable conjugation densities of camptothecin on hyaluronic acid for tumor targeting and reduction-triggered release. *Acta Biomater*. 2016;43:195–207. doi:10.1016/j.actbio.2016.07.020
- Yin S, Huai J, Chen X, et al. Intracellular delivery and antitumor effects of a redox-responsive polymeric paclitaxel conjugate based on hyaluronic acid. *Acta Biomater*. 2015;26:274–285. doi:10.1016/j.actbio.2015.08.029
- Liu Y, Qiao L, Zhang S, et al. Dual pH-responsive multifunctional nanoparticles for targeted treatment of breast cancer by combining immunotherapy and chemotherapy. *Acta Biomater*. 2018;66:310–324. doi:10.1016/j.actbio.2017.11.010
- Choi KY, Han HS, Lee ES, et al. Hyaluronic acid-based activatable nanomaterials for stimuli-responsive imaging and therapeutics: beyond CD44-mediated drug delivery. *Adv Mater*. 2019;e1803549. doi:10.1002/adma.201803549
- Qiu L, Qiao M, Chen Q, et al. Enhanced effect of pH-sensitive mixed copolymer micelles for overcoming multidrug resistance of doxorubicin. *Biomaterials*. 2014;35(37):9877–9887. doi:10.1016/j.biomaterials.2014.08.008
- Dosio F, Arpicco S, Stella B. Hyaluronic acid for anticancer drug and nucleic acid delivery. *Adv Drug Deliv Rev*. 2016;97:204–236. doi:10.1016/j.addr.2015.11.011
- Lokeshwar VB, Mirza S. Targeting hyaluronic acid family for cancer chemoprevention and therapy. *Adv Cancer Res*. 2014;123:35–65.
- Benitez A, Yates TJ, Lopez LE, et al. Targeting hyaluronidase for cancer therapy: antitumor activity of sulfated hyaluronic acid in prostate cancer cells. *Cancer Res*. 2011;71(12):4085–4095. doi:10.1158/0008-5472.CAN-10-4610
- Jordan AR, Lokeshwar SD, Lopez LE, et al. Antitumor activity of sulfated hyaluronic acid fragments in pre-clinical models of bladder cancer. *Oncotarget*. 2017;8(15):24262–24274. doi:10.18632/oncotarget.v8i15
- Isoyama T, Thwaites D, Selzer MG, et al. Differential selectivity of hyaluronidase inhibitors toward acidic and basic hyaluronidases. *Glycobiology*. 2006;16(1):11–21. doi:10.1093/glycob/cwj036
- Lim DK, Wylie RG, Langer R. Selective binding of C-6 OH sulfated hyaluronic acid to the angiogenic isoform of VEGF(165). *Biomaterials*. 2016;77:130–138. doi:10.1016/j.biomaterials.2015.10.074
- Wu JL, Liu CG, Wang XL. Preparation and characterization of nanoparticles based on histidine-hyaluronic acid conjugates as doxorubicin carriers. *J Mater Sci Mater Med*. 2012;23(8):1921–1929. doi:10.1007/s10856-012-4665-8
- Sun Y, Dai C, Yin M, et al. Hepatocellular carcinoma-targeted effect of configurations and groups of glycyrhethinic acid by evaluation of its derivative-modified liposomes. *Int J Nanomedicine*. 2018;13:1621–1632.
- Mezghrani O, Tang Y, Ke X, et al. Hepatocellular carcinoma dually-targeted nanoparticles for reduction triggered intracellular delivery of doxorubicin. *Int J Pharm*. 2015;478(2):553–568. doi:10.1016/j.ijpharm.2014.10.041
- Lv Y, Xu C, Zhao X, et al. Nanoplatform assembled from a CD44-targeted prodrug and smart liposomes for dual targeting of tumor microenvironment and cancer cells. *ACS Nano*. 2018;12(2):1519–1536. doi:10.1021/acsnano.7b08051
- Ge Z. Functional block copolymer assemblies responsive to tumor and intracellular microenvironments for site-specific drug delivery and enhanced imaging performance. *Chem Soc Rev*. 2013;42(17):7289–7325. doi:10.1039/c3cs60048c
- Venditto VJ. Cancer nanomedicines: so many papers and so few drugs! *Adv Drug Deliv Rev*. 2013;65(1):80–88. doi:10.1016/j.addr.2012.09.038
- Zhang Y, Li P, Pan H, et al. Retinal-conjugated pH-sensitive micelles induce tumor senescence for boosting breast cancer chemotherapy. *Biomaterials*. 2016;83:219–232. doi:10.1016/j.biomaterials.2016.01.023
- Zhu D, Fan F, Huang C, et al. Bubble-generating polymersomes loaded with both indocyanine green and doxorubicin for effective chemotherapy combined with photothermal therapy. *Acta Biomater*. 2018;75:386–397. doi:10.1016/j.actbio.2018.05.033
- Zhang P, Li J, Ghazwani M, et al. Effective co-delivery of doxorubicin and dasatinib using a PEG-Fmoc nanocarrier for combination cancer chemotherapy. *Biomaterials*. 2015;67:104–114. doi:10.1016/j.biomaterials.2015.07.027

32. Gupta B, Poudel BK, Ruttala HB, et al. Hyaluronic acid-capped compact silica-supported mesoporous titania nanoparticles for ligand-directed delivery of doxorubicin. *Acta Biomater.* **2018**;80:364–377. doi:10.1016/j.actbio.2018.09.006
33. Wu JL, Tian GX, Yu WJ, et al. pH-responsive hyaluronic acid-based mixed micelles for the hepatoma-targeting delivery of doxorubicin. *Int J Mol Sci.* **2016**;17(4):364. doi:10.3390/ijms17040364
34. Fu C, Li H, Li N, et al. Conjugating an anticancer drug onto thiolated hyaluronic acid by acid liable hydrazone linkage for its gelation and dual stimuli-response release. *Carbohydr Polym.* **2015**;128:163–170. doi:10.1016/j.carbpol.2015.04.024
35. Tian G, Pan R, Zhang B, et al. Liver-Targeted combination therapy basing on glycyrrhizic acid-modified DSPE-PEG-PEI nanoparticles for co-delivery of doxorubicin and Bcl-2 siRNA. *Front Pharmacol.* **2019**;10:4. doi:10.3389/fphar.2019.00004
36. Chen WL, Yang SD, Li F, et al. Programmed pH/reduction-responsive nanoparticles for efficient delivery of antitumor agents in vivo. *Acta Biomater.* **2018**;81:219–230. doi:10.1016/j.actbio.2018.09.040
37. Bao X, Wang W, Wang C, et al. A chitosan-graft-PEI-candesartan conjugate for targeted co-delivery of drug and gene in anti-angiogenesis cancer therapy. *Biomaterials.* **2014**;35(29):8450–8466. doi:10.1016/j.biomaterials.2014.06.025
38. Zhang J, Li J, Shi Z, et al. pH-sensitive polymeric nanoparticles for co-delivery of doxorubicin and curcumin to treat cancer via enhanced pro-apoptotic and anti-angiogenic activities. *Acta Biomater.* **2017**;58:349–364. doi:10.1016/j.actbio.2017.04.029
39. Wang J, Wang M, Zheng M, et al. Folate mediated self-assembled phytosterol-alginate nanoparticles for targeted intracellular anticancer drug delivery. *Colloids Surf B Biointerfaces.* **2015**;129:63–70. doi:10.1016/j.colsurfb.2015.03.028
40. Qi WW, Yu HY, Guo H, et al. Doxorubicin-loaded glycyrrhetic acid modified recombinant human serum albumin nanoparticles for targeting liver tumor chemotherapy. *Mol Pharm.* **2015**;12(3):675–683. doi:10.1021/mp500394v
41. Zhang J, Zhang M, Ji J, et al. Glycyrrhetic acid-mediated polymeric drug delivery targeting the acidic microenvironment of hepatocellular carcinoma. *Pharm Res.* **2015**;32(10):3376–3390. doi:10.1007/s11095-015-1714-2
42. Tian Q, Zhang CN, Wang XH, et al. Glycyrrhetic acid-modified chitosan/poly(ethylene glycol) nanoparticles for liver-targeted delivery. *Biomaterials.* **2010**;31(17):4748–4756. doi:10.1016/j.biomaterials.2010.02.042
43. Dai Y, Xu C, Sun X. Nanoparticle design strategies for enhanced anticancer therapy by exploiting the tumour microenvironment. *Chem Soc Rev.* **2017**;46(12):3830–3852. doi:10.1039/C6CS00592F
44. Zhang B, Wang T, Yang S, et al. Development and evaluation of oxaliplatin and irinotecan co-loaded liposomes for enhanced colorectal cancer therapy. *J Control Release.* **2016**;238:10–21. doi:10.1016/j.jconrel.2016.07.022

International Journal of Nanomedicine

Publish your work in this journal

The International Journal of Nanomedicine is an international, peer-reviewed journal focusing on the application of nanotechnology in diagnostics, therapeutics, and drug delivery systems throughout the biomedical field. This journal is indexed on PubMed Central, MedLine, CAS, SciSearch®, Current Contents®/Clinical Medicine,

Journal Citation Reports/Science Edition, EMBASE, Scopus and the Elsevier Bibliographic databases. The manuscript management system is completely online and includes a very quick and fair peer-review system, which is all easy to use. Visit <http://www.dovepress.com/testimonials.php> to read real quotes from published authors.

Submit your manuscript here: <https://www.dovepress.com/international-journal-of-nanomedicine-journal>

Dovepress